Feature Extraction for Hyperspectral Image Cubes by Noise-Adjusted Canonical Analysis

Jhe-Syuan Lai [1] and Fuan Tsai [1, 2]

[1] Department of Civil Engineering, National Central University, Taiwan
[2] Center for Space and Remote Sensing Research, National Central University, Taiwan

No. 300, Zhong-Da Rd., Jhongli, Taoyuan, Taiwan 32001;
Tel: +866(3) -422-7151 ext. 57619
E-mail: jslai0726@gmail.com; ftsai@csrsr.ncu.edu.tw

KEY WORDS: Principal component analysis, canonical analysis, minimum noise fraction, noise-adjusted canonical analysis.

Abstract:
This paper develops a novel approach that embeds minimum noise fraction (or noise-adjusted principal component analysis) in canonical analysis (called noise-adjusted canonical analysis, NACA). The objective is to take the discriminability of targets and quality of image into account simultaneously when extracting features from hyperspectral image data sets. Experimental results indicate that the NACA algorithm for classification task can produce better results than principal component analysis, conventional canonical analysis and minimum noise fraction from an airborne and an EO-1 Hyperion image data.

1. INTRODUCTION

Remote sensing techniques and materials have become popular in various applications, e.g. disaster monitoring (e.g. Sakar & Kanungo, 2004; Metternicht et al., 2005; Nichol & Wong, 2005), landuse investigation (e.g. Pacifici et al, 2009; Rozenstein & Karnieli, 2011) and environmental evaluation (e.g. Liu et al., 2002; Yang et al., 2010). For general land-cover, land-use classification tasks, multispectral images may provide adequate information to distinguish ground targets of interest. However, it may be difficult to achieve detail target detection or classification with the discrete and limited spectral information of multispectral images. Hyperspectral data, on the other hand, can supply rich spectral information for more advanced and sophisticated classifications. Nevertheless, the vast channels of hyperspectral data sets may pose a great challenge in hyperspectral image analysis. Therefore, band selection and feature extraction to reduce dimensions is often an practical necessity for effective hyperspectral image analysis and applications..

Principal component analysis (PCA) is a popular transformation to mitigate the drawbacks of high-dimensionality, e.g. Hughes phenomenon (Hughes, 1968) and redundancy. The criterion of PCA is based on maximum covariance. However, this type of band- or global-based computation may not provide helpful and detailed discriminability between different surfaces (Cheriyadat & Bruce, 2003; Goldberge et al., 2007). Furthermore, it does not consider image quality (Chang & Du, 1999). On the other hand, canonical analysis (CA) is similar to PCA but the covariance is calculated according to within and among classes. It can provide the distinction of class-pair for better target recognition. Nevertheless, it does not take the quality of image into account when computing the class separability. Consequently, the results may not be good enough for classification. Minimum noise fraction (MNF) or noise-adjusted principal component analysis (NAPCA) is another transformation which depends on signal to noise ratio (SNR). The results of MNF can reflect image quality. Hence, this paper develops a novel approach for feature extraction that embeds the MNF concept in CA (called noise-adjusted canonical analysis, NACA) to take the discriminability of targets and image quality into account at the same time for effective feature extraction of hyperspectral images.

2. PROPOSED METHOD

There are two steps in NACA in order to consider image quality and classes' separability simultaneously. First, the MNF algorithm is performed to reduce noise by band selection. Consequently, applying CA operator to previous results enhances discriminability between different classes. For the band selection, this study finds the convergence band from MNF egienvalue diagram (see Figure 1, the convergence is band 6 in this case). Then the first principal

band to convergence band (which are assumed signal only) is inputted in the CA approach. Finally, the front bands of CA results indicate the extracted information have good image quality and separability.

The concept of MNF is to calculate covariance of the entire image and noise and produce SNR by the whiten technique (Eq. (1)). Then PCA is performed to obtain eigenvalues and eigenvectors (Eq. (2)) as discussed in Chang & Du (1999). On the other hand, CA computes the covariances of within (Eq. (3)) and among classes (Eq. (4)), and then solves the eigenvalues and eigenvectors.

Table 1 shows the methods comparison between PCA, CA, MNF and NACA algorithms, where V and λ are the eigenvector and eigenvalue matrix; Σ indicates the covariance matrix of the image; Σ_{Among} and Σ_{Within} represent the covariance matrix of among and within classes; Σ_{Noise} marks the covariance matrix of noise. It is obvious that NACA combines SNR, PCA (MNF) and CA concepts to extract useful and quality information.

$$F = E\Delta_n^{-1/2} \quad (1)$$

$$H = GF \quad (2)$$

where
F: noise-whitening matrix
E: a transform
Δ_n : diagonal eigenvalue matrix of the noise covariance
H: MNF result
G: eigenvector matrix from a PCA based on noise-adjusted data covariance

$$\Sigma_{Within} = \frac{1}{M}\Sigma_{i=1}^{M}\Sigma_i \quad (3)$$

$$\Sigma_{Among} = \xi\{(m_i - m_0)(m_i - m_0)\}^t \quad (4)$$

where
Σ_{Within} : covariance matrix of within class
M: number of classes
Σ_i : covariance matrix of the data in class i
Σ_{Among} : covariance matrix of among class
m_i : mean of ith class
m_0 : global mean

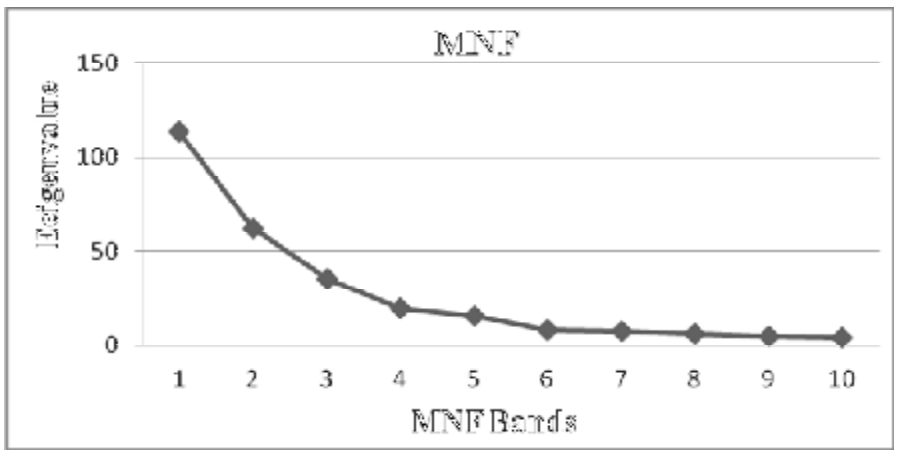

Figure 1: MNF band selection by eigenvalue diagram (only shows top 10; the convergence is band 6)

Table 1: Methods comparison

Methods	Criterion	Tool	Reference
PCA	[V, λ]= Eig (Σ)	ENVI	(Richards, 1999)
CA	[V, λ]= Eig (Σ_{Among}, Σ_{Within})	Matlab	-
MNF	[V, λ]= Eig (Σ_{Noise}/ Σ) ➔ PCA	ENVI	(Green et al., 1988)
NACA	MNF ➔ CA	ENVI+Matlab	-

3. DATA & RESULTS

Two hyperspectral image cubes (Intelligent Spectral Imaging System, ISIS, and EO-1 Hyperion, see Figure 2) were used to test the developed algorithms. The properties of the datasets are displayed in Table 2. Because some bands in the two datasets are nosier, null information, low SNR or redundancy, some of the spectral bands were excluded from the analysis. As a result, there are 160 (522.8- 902.7 nm) and 95 (426.82- 2395.5 nm) bands remained for ISIS and Hyperion cases (Tsai et al., 2007a; Tsai et al., 2007b). The number of pixels of training and check data are shown in Table 3.

Because the goal of PCA, CA, MNF and NACA is to extract and sort useful information. These first and second principal bands are very important. The images are classified into different classes (as listed in Table 3) based on the extracted principal bands and using maximum likelihood classifier (threshold is 0.95). The evaluations of the classifications, including the PA (Producer Accuracy), UA (User Accuracy), OA (Overall Accuracy) and kappa coefficient, are discussed in the subsequent sections for both the ISIS and Hyperion cases.

ISIS (R: 663.8 nm, G: 561.0 nm, B: 501.3 nm) Hyperion (R: 660.85 nm, G: 559.09 nm, B: 487.87 nm)

Figure 2: Test images and ground truth

Table 2: Image properties

Data source	ISIS (used)	Hyperion (used)
Location	Xi-Tou, Taiwan	Heng-Chun, Taiwan
Date	September, 2006	January, 2004
Platform	Airborne	Spaceborne (EO-1)
Image size (pixels)	1200×400	481×256
Spatial resolution (m)	1.5	30
Spectral resolution (nm)	3.5- 5	10

Spectral range (nm)	430- 945 (522.8- 902.7)	355- 2577 (426.82- 2395.5)
Number of band	218 (160)	242 (95)

Table 3: Number of pixels of training and check data (the words' color correspond with Figure 1)

ISIS	Building	Road	Land	Grass	Farmland	Coniferous Forest	Bamboo
Training	2015	1456	571	2746	2087	3369	2453
Check	182	274	82	223	119	439	342
Hyperion	Building	Water	Land	Grass	Taiwan Acacia	Negundo Chastetree	Leucaena Leucocephala
Training	60	70	75	70	193	111	139
Check	30	39	46	39	115	64	90

3.1. ISIS Case

Figure 3 shows the MNF eigenvalue diagram. It is clear that the convergence is band 7. Therefore, the first to the seventh bands are inputted in CA algorithm. Figure 4 displays the top 2 principal component of PCA, CA, MNF and NACA. For the classification comparison, the PA, UA, OA and kappa evaluations are shown in Table 4. It appears that CA and NACA produce better results than PCA and MNF. In addition, there are many pixels of PCA whose probability after MLC classification is less than 0.95. Those were identified as the unclassified pixels and resulted in very poor classification results. In general, the discriminability-based strategy produced better results than MNF mechanism in this case.

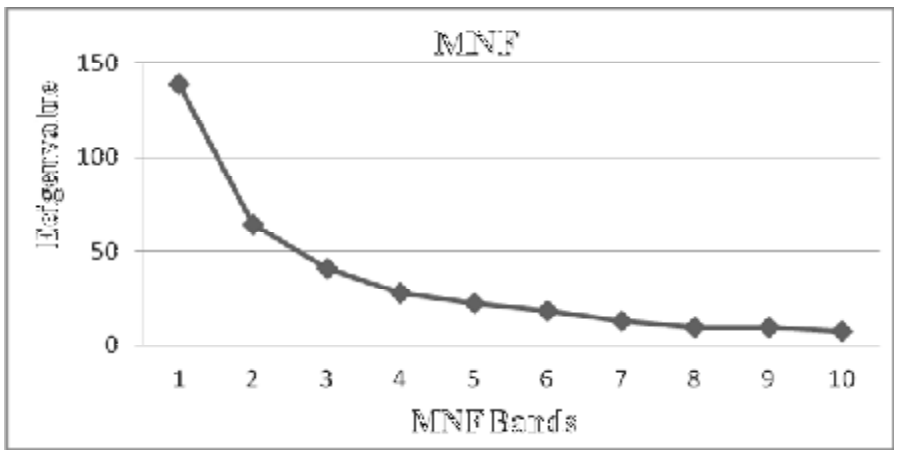

Figure 3: The MNF eigenvalue diagram in ISIS case (only show top 10, the convergence is band 7)

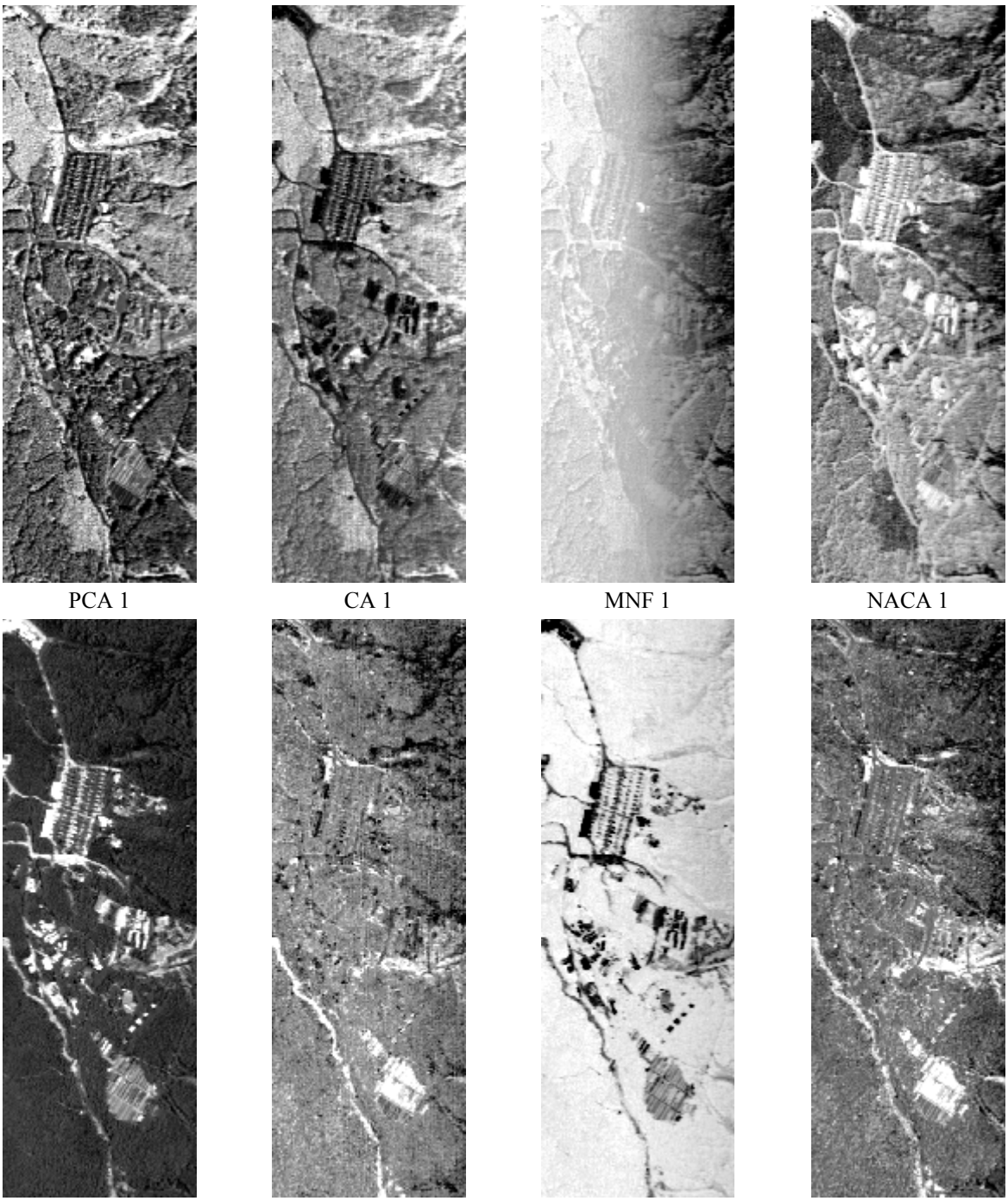

Figure 4: First and second principal images in ISIS case

Table 4: Classification results in ISIS case

Classes		PCA	CA	MNF	NACA
Building	PA (%)	0	80.22	81.32	64.84
	UA (%)	0	85.88	96.1	85.51
Road	PA (%)	0	70.85	50.22	62.33
	UA (%)	0	59.18	56.85	58.4
Land	PA (%)	0	74.09	63.14	73.72
	UA (%)	0	73.82	86.93	68.71
Grass	PA (%)	0	68.29	80.49	79.27
	UA (%)	0	80	35.87	61.32

Farmland	PA (%)	0	63.87	84.03	73.95
	UA (%)	0	55.07	75.76	83.02
Coniferous Forest	PA (%)	28.7	78.36	70.84	80.87
	UA (%)	96.92	82.49	73.35	82.75
Bamboo	PA (%)	35.67	65.5	59.06	69.3
	UA (%)	73.49	69.14	54.45	67.71
OA (%)		14.93	72.67	66.95	72.49
Kappa		0.1127	0.6688	0.6016	0.6657

3.2. Hyperion Case

Similar test was also performed on the Hyperion image cube. In this test, top 6 of MNF bands were used to perform CA operator as displayed Figure 5. Figure 6 listed the first and second principal components of feature extraction by the four approaches. A quick visual comparison of the four transformations in this case indicates that NACA images provide better quality than CA and discriminability than PCA and MNF. To further evaluate the classification, the best results were generated from NACA. Comparing Figure 4 and Figure 6, it is noticed that the quality of Hyperion image is worse than ISIS dataset. However, NACA still produced the best classification results among the four methods of feature extraction. It further proves that NACA considers image quality and separability of targets simultaneously and can better extract truly discriminant features from the data sets.

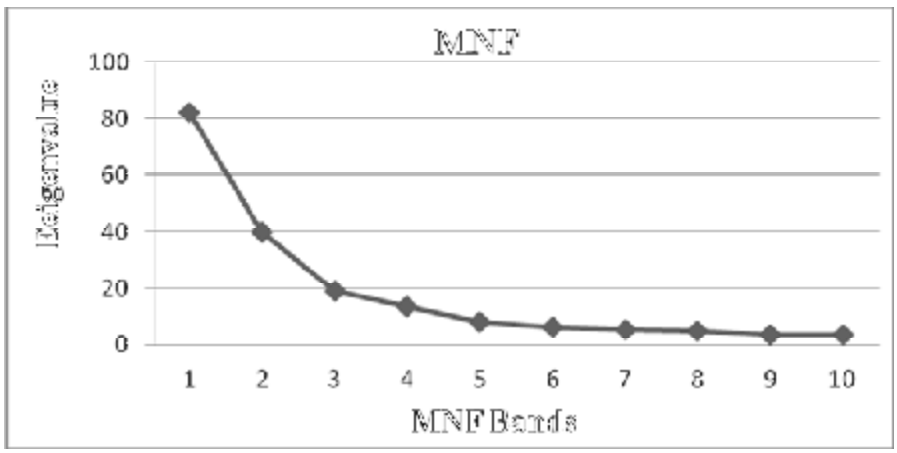

Figure 5: The MNF eigenvalue diagram in Hyperion case (only show top 10, the convergence is band 6)

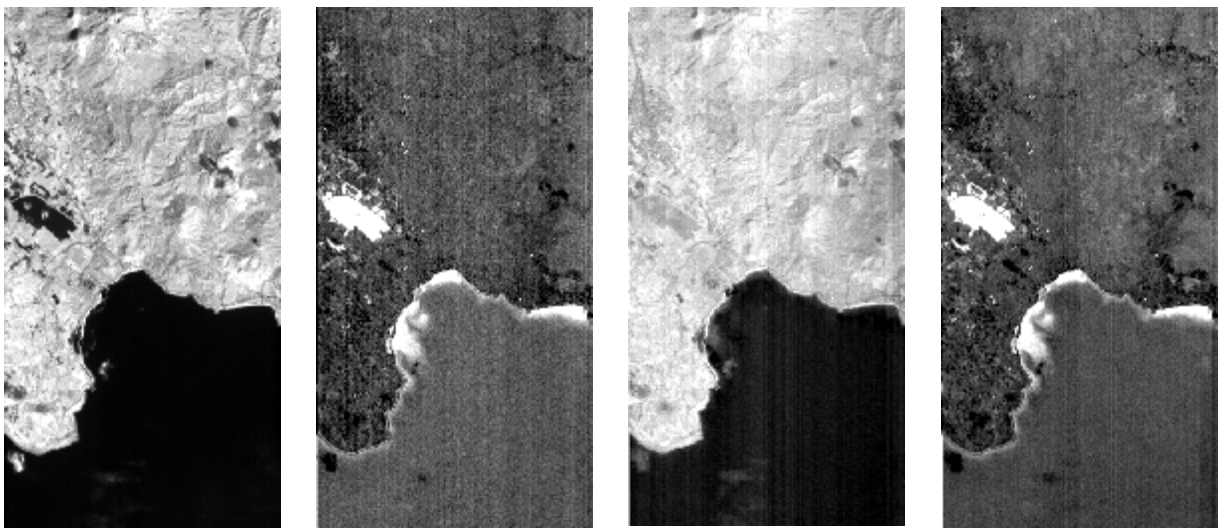

PCA 1 CA 1 MNF 1 NACA 1

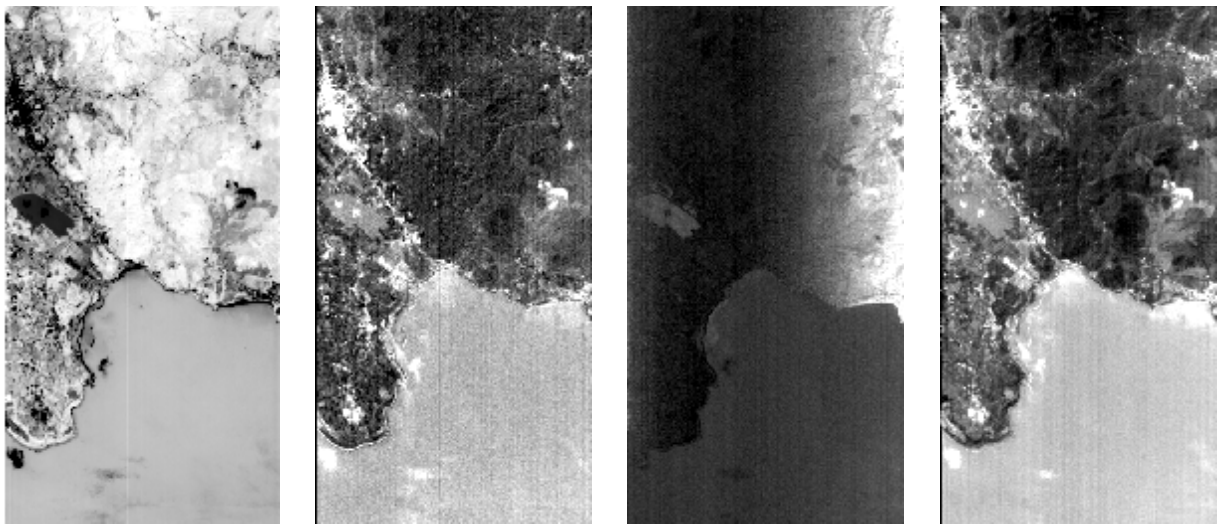

PCA 2 CA 2 MNF 2 NACA 2

Figure 6: First and second principal images in Hyperion case

Table 5: Classification results in Hyperion case

Classes		PCA	CA	MNF	NACA
Building	PA (%)	0	100	53.33	100
	UA (%)	0	100	48.48	100
Water	PA (%)	94.74	100	94.74	100
	UA (%)	100	100	90	100
Land	PA (%)	0	58.97	74.36	76.92
	UA (%)	0	48.94	58	78.95
Grass	PA (%)	0	91.3	47.83	95.65
	UA (%)	0	71.19	64.71	88
Taiwan Acacia	PA (%)	70.43	53.04	67.83	80
	UA (%)	88.04	59.8	71.56	76.67
Negundo Chastetree	PA (%)	64.06	53.13	64.06	81.25
	UA (%)	66.13	45.33	48.81	54.17
Leucaena Leucocephala	PA (%)	18.89	45.56	64.44	34.44
	UA (%)	62.96	57.75	80.56	62
OA (%)		41.47	63.74	66.35	75.12
Kappa		0.3475	0.5645	0.5942	0.6996

4. CONCLUSIONS & FUTURE WORKS

This study proposed a novel algorithm (noise-adjusted canonical analysis, NACA) to reduce dimensionality and extract useful features from hyperspectral images for classification. Two test cases demonstrated the NACA can preserve not only image quality but discriminability between targets. The results of all experiments are evaluated the PA, UA, OA and kappa measures. In all evaluations, NACA has better accuracy on both the ISIS and Hyperion image cubes.

Currently, NACA is just a hierarchical strategy, i.e. performing MNF and then CA. Future work will integrate noise estimation and CA together to generate a more coherent, efficient and systematic algorithm.

REFERENCES:

Chang, C. -I. and Du, Q., 1999. Interference and noise-adjusted principal component analysis. IEEE Transactions on Geoscience and Remote Sensing, 37(5), pp. 2387-2396.

Cheriyadat, A. and Bruce, L. M., 2003. Why principal component analysis is not an appropriate feature extraction method for hyperspectral data. Proceeding 2003 IEEE Geoscience and Remote Sensing Symposium, pp. 3420-3422.

Goldberg, H., Kwon, H. and Nasrabadi, N. M., 2007. Kernel eigenspace separation transform for subspace anomaly detection in hyperspectral imagery. IEEE Geoscience and Remote Sensing Letters, 4(4), pp. 581-585.

Green, A. A., Berman, M., Switzer, P. and Craig, M. D., 1988. A transformation for ordering multispectral data in terms of image quality with implications for noise removal. IEEE Transactions on Geoscience and Remote Sensing, 26(1), pp. 65-74.

Hughes, G. F., 1968. On the mean accuracy of statistical pattern recognition. IEEE Transactions on Information Theory, 14, pp. 55-63.

Liu, G. -R., Lin, T. -H. and Kuo, T. -H., 2002. Estimation of aerosol optical depth by applying the optimal distance number to NOAA AVHRR data. Remote Sensing of Enviroment, 81, pp. 247-252.

Mettemicht, G., Hurni, L. and Gogu, R., 2005. Remote sensing of landslides: An analysis of the potential contribution to geo-spatial systems for hazard assessment in mountainous environments. Remote Sensing of Environment, 98, pp. 284-303.

Nichol, J. and Wong, M. S., 2005. Satellite remote sensing for detailed landslide inventories using change detection and image fusion. International Journal of Remote Sensing, 26(9), pp. 1913-1926.

Pacifici, F., Chini, M. and Emery, W. J., 2009. A neural network approach using multi-scale textural metrics from very high-resolution panchromatic imagery for urban land-use classification. Remote Sensing of Environment, 113(6), pp. 1276-1292.

Richards, J. A., 1999. Remote sensing digital image analysis: An introduction. Springer-Verlag, Berlin, Germany, pp. 240.

Rozenstein O. and Karnieli, A., 2011. Comparison of methods for land-use classification incorporating remote sensing and GIS input. Applied Geography. 31, pp. 533-544.

Sakar, S. and Kanungo, D. P., 2004. An integrated approach for landslide susceptibility mapping using remote sensing and GIS. Photogrammetric Engineering & Remote Sensing, 70, pp. 614-625.

Tsai, F., Chang, C. -K., Rau, J. -Y., Lin, T. -H. and Liu, G. -R., 2007a. 3D computation of gray level co-occurrence in hyperspectral image cubes. Lecture Notes in Computer Science, 4679, pp. 429-440.

Tsai, F., Lin, E. -K. and Yoshino, K., 2007b. Spectrally segmented principal component analysis of hyperspectral imagery for mapping invasive plant species. International Journal of Remote Sensing, 28(5-6), pp. 1023-1039.

Yang, G., Pu, R., HuangW., Wang, J. and Zhao, C., 2010. A novel method to estimate subpixel temperature by fusing solar-reflective and thermal-infrared remote-sensing data with an artificial neural network. IEEE Transactions on Geoscience and Remote Sensing, 48(4), pp. 2170-2178.